

# Fluctuation Measurement in Electron Penetration Experiment on Helical Magnetic Configuration

WAKABAYASHI Hidenori, HIMURA Haruhiko, FUKAO Masayuki,  
ISOBE Mitsutaka<sup>1</sup>, YOSHIDA Zensho and the CHS group<sup>1</sup>  
*The University of Tokyo, Graduate School of Frontier Sciences, Tokyo, 113-0033, Japan*  
<sup>1</sup>*National Institute for Fusion Science, Toki, 509-5292, Japan*

(Received: 12 December 2003 / Accepted: 11 March 2004)

## Abstract

Experimental studies on collisionless penetration of electrons into helical magnetic surfaces (HMS) via stochastic magnetic region (SMR) have been performed on the Compact Helical System device. For the case where the magnetic axis is located at 101.6 cm and the beam density  $n_b$  of electrons is more than  $\sim 10^{13} \text{ m}^{-3}$ , some electrons move across the last closed flux surface and penetrate significantly into the HMS by a collisionless process. In order to investigate the detailed mechanism of the collisionless electron penetration, measurements of magnetic fluctuations have been conducted in the HMS and SMR. When  $n_b$  is larger than  $\sim 10^{13} \text{ m}^{-3}$ , a magnetic probe shows apparent fluctuations of about 3 MHz.

## Keywords:

helical non-neutral plasma, electron penetration, stochastic magnetic region

## 1. Introduction

There are many experimental, theoretical, and computer studies of cross-field plasma propagation in several research areas such as the penetration of solar wind into the geomagnetic field [1], plasma-beam injection into a magnetic containment device [2], inward turbulent particle transport in helical plasmas [3], injection of energetic electrons into toroidal plasmas to control electric fields [4], and recently, electron penetration into closed magnetic surfaces via stochastic magnetic region (SMR) [5].

In the experiment, when the SMR is present, some field-following electrons in the SMR move into the helical magnetic surfaces (HMS) across the last closed flux surface (LCFS) of a stellarator configuration. However, it is never observed for cases where the SMR is lost, nor is the density of the injected electrons small ( $n_b < 10^{13} \text{ cm}^{-3}$ ) in the SMR. Another significant feature of the inward propagation of the injected electrons is that the penetration occurs in 100  $\mu\text{s}$  which is much shorter than all collision times; for typical experimental parameters of the experiment, the electron-electron and electron-neutral collision times are 1 s and 4 ms, respectively. This means that the observed penetration is caused by a collisionless process. No dependence on the pitch angle between the injected electrons and the magnetic field is observed. In fact, all possible orbital motion of the injected electrons outside the LCFS never extend inside the LCFS [6]. These suggest the existence of cross-field transport that is

associated with free-streaming of electrons along the stochastically wandering field lines in the SMR. In order to investigate the detailed mechanism of the collisionless electron penetration, magnetic fluctuations have been conducted in the HMS and SMR.

In this paper, we present the data of magnetic fluctuations observed during the collisionless electron penetration. In Sec. 2, we explain the experimental setup of this experiment. In Sec. 3, we briefly explain the collisionless electron penetration with a typical set of probe current measured in the HMS. The first experimental data of fluctuations are discussed in Sec. 4.

## 2. Experimental setup

Experiments are conducted on the Compact Helical System [7]. A schematic drawing of the experimental setup is shown in Fig. 1. CHS is a medium-size stellarator device whose major ( $R$ ) and average minor radii ( $\bar{r}$ ) are 1.0 and 0.2 m, respectively. The aspect ratio is thus about 5, which is relatively lower than other conventional stellarator devices. The pole and toroidal period numbers of the helical field coils of the device are 2 and 8, respectively.

On CHS, there are two key parameters which identify the helical magnetic configuration. One of these is position of the magnetic axis ( $R_{ax}$ ), which is defined by the radial position of the magnetic axis on a vertical cross section and

is usually set around 92.1 cm [8]. For this setting, inner edge of the HMS intersects the vacuum chamber [5]. This results

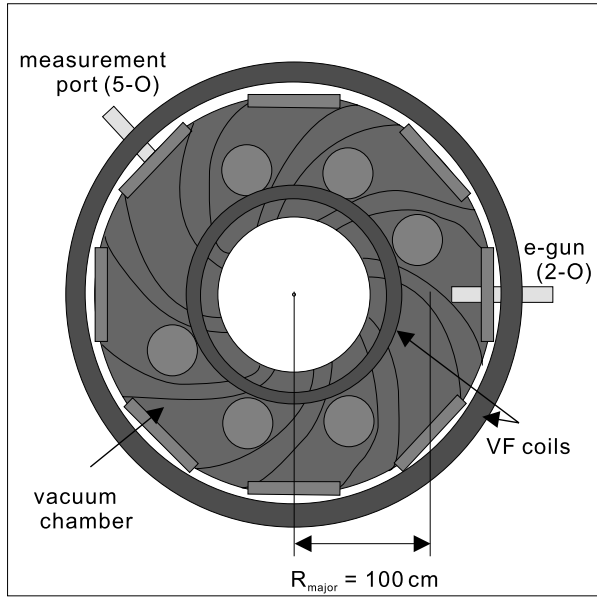


Fig. 1 A schematic drawing of the CHS device, the electron gun (e-gun) and the measurement port. The e-gun and measurement probes are inserted horizontally on 2-O and 5-O ports, respectively.

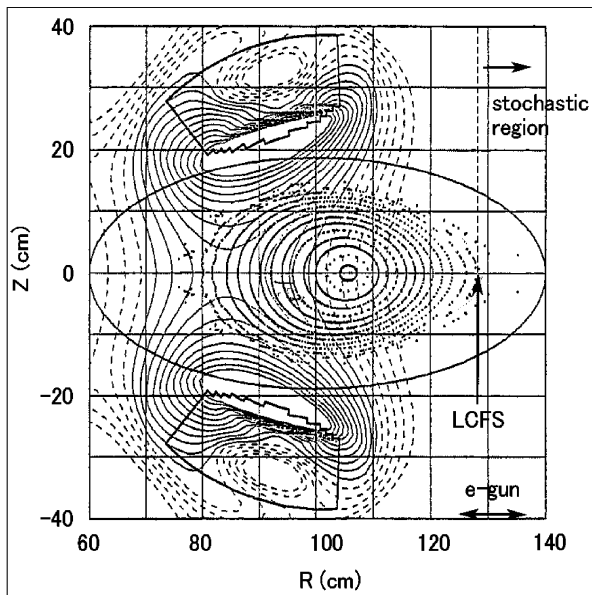


Fig. 2 A poloidal cross section of the CHS device drawn with Poincare plots of the magnetic field lines. This is a horizontal cross section which corresponds to 5-O port of the actual device where the probes are inserted (Fig. 1). Helical magnetic surfaces are recognized as nested surface structures between the magnetic axis and the last closed flux surface (LCFS). The LCFS is at  $R = 128$  cm on the equatorial plane and the stochastic magnetic region exists surrounding the magnetic surfaces. In this figure the magnetic axis seems to be located around  $R = 106$  cm due to weak helical winding of the magnetic axis itself, although  $R_{ax}$ , which is defined on a vertical cross section, is 101.6 cm on this configuration.

in breaking of the SMR. When  $R_{ax}$  is shifted outward and fixed at 101.6 cm, the HMS does not touch the chamber as seen in Fig. 2. Thus, the SMR surrounding the HMS is present. The second key parameter is the strength of  $\mathbf{B}$ . The typical strength of  $\mathbf{B}$  is 0.9 kG, which yields an electron gyroradius of approximately 1.3 mm when maximum speed of electrons is assumed to be about  $2 \times 10^7$  m/s where the beam energy ( $eV_{acc}$ ) is about 1.2 keV.

Electrons are injected from a typical diode-type electron gun (henceforth called e-gun) which uses a  $\text{LaB}_6$  emitter as the cathode. The shape of the cathode is quadrate (1.5 cm each) and the emitter has also a quadrille shape with tungsten wires. Value of beam current ( $I_b$ ) and  $eV_{acc}$  of the injected electrons can be varied. The maximum value of  $I_b$  for the presented experiment is  $\sim 400$  mA at the cathode temperature  $\sim 2000$  K. Also, the maximum value of  $eV_{acc}$  is  $\sim 1.2$  keV, where the anode and cathode potentials are 0 and  $-1.2$  kV, respectively. The e-gun is installed in the equatorial plane ( $z = 0$ ) and the cathode is placed in the SMR. The toroidal angle ( $\phi$ ) of the poloidal plane where the e-gun is placed is defined as  $0^\circ$ . The e-gun can also be moved along the  $r$  axis and rotated around its barrel to vary the injection angle of the emitted electrons.

For diagnostics, we have employed two probes. One of those work as not only an electrostatic probe but also an emissive probe [9]. The probe tip is made of a Thoriated-tungsten (1% Th-W) wire with  $\phi 0.15$  mm. The surface area of the filament is  $8.2$  mm<sup>2</sup>. With the probe, both space potential ( $\phi_p$ ) and  $I_p$  are measured. The probe is inserted along the  $r$ -axis at the #5 ( $\phi = 205^\circ$ ), as recognized in Fig. 1. The second one is a pick-up coil which is made of a copper wire with  $\phi 0.2$  mm. The coil has ten turns with diameter of 3.3 mm, which can be applied to measure up to  $\sim 20$  MHz of magnetic fluctuations. Those two probes are movable, which provides spatial distribution of  $I_p$  and  $dB/dt$ .

### 3. Collisionless electron penetration

Substantial penetration of the injected electrons is observed [5]. Figure 3 shows time evolution of  $I_p$  after the electron injection. Electrons are launched in the SMR, 2 cm outside the LCFS. The  $\sqrt{\Psi} = 0$  and 1 of the horizontal axis correspond to  $R_{ax}$  and the LCFS, respectively. Though the e-gun is placed in the SMR (at  $\sqrt{\Psi} \sim 1.1$ ), finite value of  $I_p$  are clearly measured even inside the LCFS ( $\sqrt{\Psi} < 1$ ). As clearly seen in Fig. 3, the  $I_p$  data significantly increase in  $\sim 100$   $\mu$ s and almost saturate in  $\sim 1$  ms inside the HMS, which indicates that the electron penetration happens in  $\sim 100$   $\mu$ s and continues. This value of  $\delta t \sim 100$   $\mu$ s is much faster than the electron-neutral collision time,  $\tau_{en}$ , which is calculated to be  $\sim 4$  ms for  $v_e \sim 10^7$  m/s and  $P_0 \sim 5 \times 10^{-8}$  Torr, where  $P_0$  is the background vacuum pressure. The length scale,  $\delta l$ , of penetration is approximately equal to the length of  $\bar{r}$  because the penetrated electrons have reached  $R_{ax}$  in  $\delta t$ . Since  $\rho_e$  is  $\sim 2$  mm as already explained,  $\delta l$  is thus about 100 times as long as  $\rho_e$ . These results indicate that the observed penetration of electrons is caused by a collisionless process.

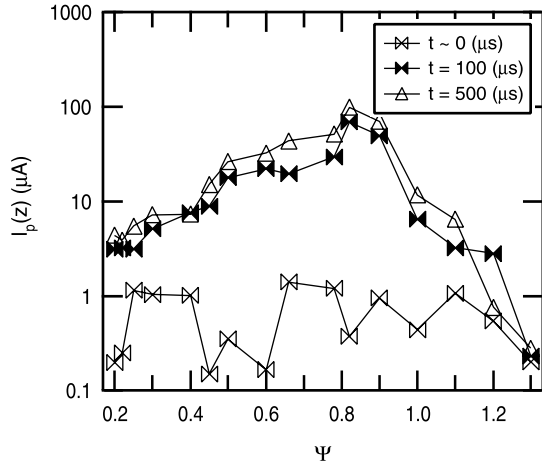


Fig. 3 Time evolution of a typical profile of probe current measured along the  $z$  axis at #6. Electrons are injected in the stochastic region, which is outside the last closed flux surface (LCFS). Nevertheless, electrons penetrate inside the LCFS.

#### 4. Measurements of magnetic field fluctuation

Figure 4 shows time series of magnetic fluctuation measured on the LCFS by the pickup-coil at #5. Two panels correspond to emission beam density  $n_b =$  (a)  $3.5 \times 10^{12} \text{ m}^{-3}$  and (b)  $2.5 \times 10^{13} \text{ m}^{-3}$ , respectively. In these cases, electrons are continuously emitted from the e-gun during  $t = 0 \mu\text{s}$  and  $300 \mu\text{s}$ . According to the preliminary results of space potential and electron flux measurements, no electron penetration takes place in case (a) and the penetration grows as  $n_b$  becomes larger, until it saturates when  $n_b \sim 10^{13} \text{ m}^{-3}$ . So, in case (b) a significant penetration takes place in the HMS.

Figure 5 shows time evolution of FFT spectrum of measured magnetic fluctuation, divided into each  $50 \mu\text{s}$ . Panels (a) and (b) correspond to two cases of Fig. 4. In panel (a) which is the no penetration case, we can recognize almost no oscillation in the beginning of the injection ( $\sim 100 \mu\text{s}$ ). And in the later part of the injection, broad spectrum between 20 MHz and 40 MHz are recognized. These fast oscillations are also observed in the significant penetration case (panel (b)). On the other hand, in panel (b), a 3 MHz peak and its higher harmonics can be found in the beginning of a shot ( $t \sim 0 - 100 \mu\text{s}$ ) and they decrease in the later part ( $100 \mu\text{s} \sim$ ). This duration of  $100 \mu\text{s}$  seems to be in a good agreement with the measurements already mentioned in the previous section.

Comparing these results, it is possible that the 3 MHz oscillation reflects some instability related to the penetration process of electrons into the HMS because it is found only in the beginning of the shots in which the penetration takes place. And the faster oscillation seen in both penetrating and no-penetrating shots can be some beam related oscillations.

The observation of the magnetic fluctuation implies a possibility of destruction of magnetic surfaces in the vicinity of the LCFS. In fact, according to the numerical analyses of the magnetic field, the magnetic surfaces around the LCFS

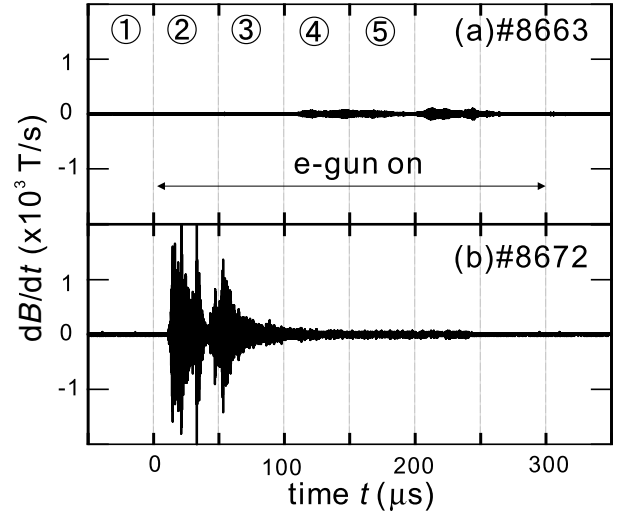


Fig. 4 Time series of magnetic field fluctuation measured on the LCFS. Electrons are continuously injected during  $t = 0 \text{ ms}$  and  $300 \mu\text{s}$ . Two panels correspond to emission beam electron density  $n_b =$  (a)  $3.5 \times 10^{12} \text{ m}^{-3}$  and (b)  $2.5 \times 10^{13} \text{ m}^{-3}$ , respectively. According to flux measurements, no penetration takes place in case (a) and a significant penetration occurs in case (b).

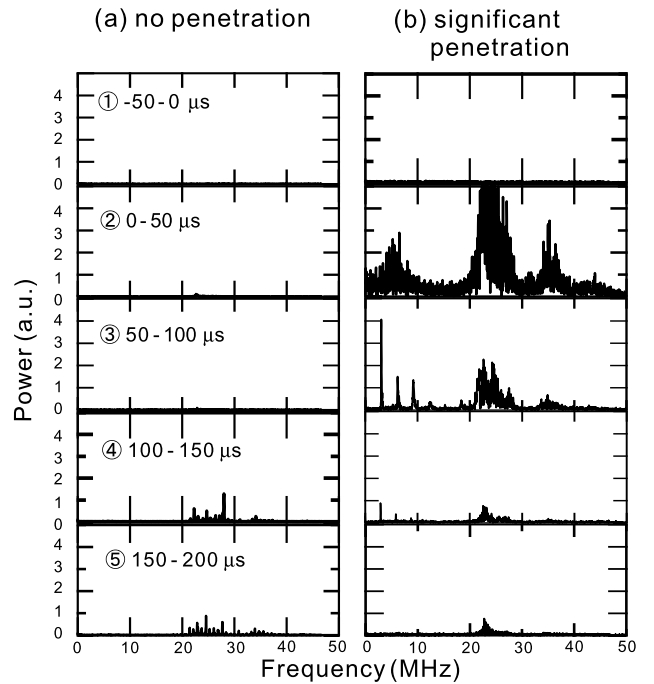


Fig. 5 Time evolution of FFT spectrum of (a) no penetration case (#8663) and (b) significant penetration case (#8672). Panels ①–⑤ correspond to each  $50 \text{ ms}$  duration of Fig. 5, where electron injection begins at  $t = 0 \text{ ms}$ . Broad spectrum between 20 and 40 MHz are recognized in both cases. However, 3 MHz peak and its higher harmonics are observed only in panels (b) ②–④, which correspond to the beginning of the significant penetration of electrons.

are very fragile and can easily be destructed even by perturbation of 0.1 %. If the perturbation of the magnetic field destructs the magnetic surfaces, it is likely that electrons can get into the destructed magnetic surfaces. However, that does not completely explain the observation that electrons can penetrate into near the magnetic axis.

## 5. Summary

We have performed experiments of electron injection into the helical magnetic surfaces, and observed that injected electrons penetrate deeply inside the magnetic surfaces. The penetration process is collisionless and collective phenomena because it takes place in a time scale much faster than any collision time and the beam electron density is the key parameter of the penetration process. In order to investigate the mechanism of the process, magnetic field fluctuations have been measured to find 3 MHz oscillations, which can only be recognized during the penetration. To clarify the mechanism, further investigations such as parameter dependence of the frequency of the fluctuation are needed.

## Acknowledgements

This research has been conducted since August, 2001 with the support and under the auspices of the NIFS LHD Project Research Collaboration. HW is also supported by Futaba Electric Corporation Foundation.

## References

- [1] W. Dai *et al.*, Phys. Plasmas **2**, 1725 (1995).
- [2] F.J. Wessel *et al.*, Phys. Fluids B **2**, 1467 (1990); L. Lindberg, Astrophys. Space Sci. **55**, 203 (1978).
- [3] K. Ohkuni *et al.*, Phys. Plasmas **8**, 4035 (2001).
- [4] O. Motojima *et al.*, Nucl. Fusion **40**, 833 (2000).
- [5] H. Himura, H. Wakabayashi *et al.*, Phys. Plasmas **11**, 492 (2004).
- [6] H. Wakabayashi, H. Himura *et al.*, *Non-Neutral Plasma Physics V* (American Institute of Physics, New York, 2003) p. 332.
- [7] K. Matsuoka *et al.*, Plasma Phys. Control. Fusion **42**, 1145 (2000).
- [8] M. Isobe *et al.*, Rev. Sci. Instrum. **70**, 827 (1999).
- [9] H. Himura *et al.*, Rev. Sci. Instrum. **74**, 4658 (2003).